We are IntechOpen, the world's leading publisher of Open Access books Built by scientists, for scientists

4,800
Open access books available

122,000
International authors and editors

135M
Downloads

Our authors are among the

154
Countries delivered to

TOP 1%
most cited scientists

12.2%
Contributors from top 500 universities

CLARIVATE ANALYTICS BOOK CITATION INDEX INDEXED

WEB OF SCIENCE™

Selection of our books indexed in the Book Citation Index in Web of Science™ Core Collection (BKCI)

Interested in publishing with us?
Contact book.department@intechopen.com

Numbers displayed above are based on latest data collected.
For more information visit www.intechopen.com

2

Design of Stereo Omni-directional Vision Sensors with Full Sphere View and without Dead Angle

Tang Yi-ping, Lin Bei, Chen Min-zhi and Sun Jun
Zhejiang University of Technology
China

1. Introduction

As the sensor technology and image processing technology rapidly developped, more and more scholars have paid attention to the panoramic imaging technology. Panoramic imaging technology can be applied to military, medicine, security, etc. Panoramic imaging technology has became an important research topic in the field of computer vision. There are four current methods to obtain panoramic images which are rotation imaging, multi-camera imaging, fish-eye lens imaging and catadioptric imaging. This chapter explores the existing panoramic imaging technology, proposes improved ideas and methods to the original ODVS, which are average angular resolution and second catadioptric imaging technology, and achieves 360°×360° full sphere panoramic image by integrating two images acquired by two symmetrical ODVSs. Experiments confirm that this method can obtain a sphere view field and has important application value in field of video surveillance.

2. Related research

Herman and other scholars, rotated camera around the fixed axis which was perpendicular to the optical axis to shoot multiple image by rotation imaging technology, then stitched these images together to obtain panoramic image. But this method is time-consuming, and dose not meet the real-time requirement. Multi-camera imaging is shown in Fig. 1, the U.S. IMC company have developed multi-camera imaging device wihich uesd a number of cameras capturing images facing different directions, and stitched these images to get panoramic image. Fig. 1(a) is a hemispherical ODVS composed of multi-camera, and this device can obtain video images within a half-sphere; Fig. 1(b) is a sphere ODVS composed of multi-camera, and this device can obtain video images within the entire sphere. The cost of multi-camera device is high, the stitching algorithm is time-consuming, and the computational cost of the implemention of video data fusion is high. Another way to obtain panoramic image is fish-eye, but this approach requires a very short focus, and the vision of the imaging system can be expanded to half sphere or more. However, this imaging technology introduces image distortion, whose model does not meet the perspective projection requirements and could not get the undistorted perspective projection image by the acquired images. In addition, the resolution of the image is uneven and the fish-eye is

expensive. Catadioptric ODVS is composed of a CCD camera and a mirror facing the camera. In the horizontal direction, the viewing angle range is 360°, while in the vertical direction there is a blind angle about 120°. KoyasuH has used a pair of hyperbolic mirrors and a projection lens to compose a panoramic vision system, but there was still inherent dead angle. Zhu Feng the researcher of China's Shenyang Institute of Automation also has carried out pioneering research work in this area, and proposed design method with an ordinary camera to achieve omnidirectional stereo vision. This device is low cost, but one of the panoramic video is vague due to shooting two panoramic video images of catadioptric mirror with different depths only by one video camera, and it is still difficult to obtain full sphere panoramic video image without dead angle.

(a) Hemisphere camera device (b) Full sphere camera device

Fig. 1. Multi-camera ODVS device

Viewing deficiencies in the designed system above, this chapter presents a full sphere ODVS structure. It can obtain the sphere panoramic image with the advantages of convenience, real-time processing, novelty, low cost. Work to be done first is to design a kind OVDS with average angular resolution so as to stitching the two ODVS seamlessly later, followed is to analyse the dead angle of the original ODVS in vertical direction to improve the ODVS structure, and then is to stitch 360°×360° video image seamlessly by unwrapping algorithm to achieve a 360°×360° sphere ODVS.

3. Design of the sphere 360°×360°ODVS

3.1 Design of the ODVS structure

The first work is to design ODVS with no dead angle, which can sense all points on hemispherical surface in real-time, and its view scope is the same as the hemisphere device in Fig. 1(a). Omnidirectional vision device is shown in Fig. 2. The second is to configure the camera behind the hyperbolic mirror. The camera's lens fixed at the single view point (SVP) of the catadioptric mirror. There is a small hole at the center of firstly reflection mirror through which camera shoots video information before the firstly reflection mirror; in front of firstly reflection mirror equips a secondary reflection mirror, at the center of which there is also a small hole with a embedded wide-angle lens; omni-directional video information first reflects by firstly reflection mirror, then secondly reflects by secondary reflection mirror, and then through the small hole in firstly reflection mirror images in camera device; in addition, the projects in front of the firstly reflection mirror through the wide-angle lens image between the wide-angle lens and the camera lens, known as the first imaging point, the image point through the small hole in firstly reflection mirror images at the focus of the lens of camera imaging component. This design of ODVS eliminates the dead angle before secondary reflection mirror.

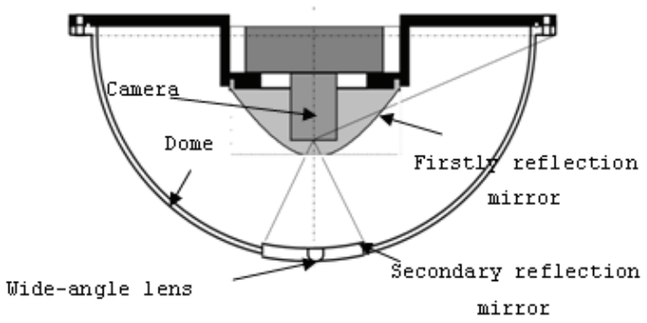

Fig. 2. Structure of ODVS without dead angle

As shown in Fig. 2, we obtain real-time 360°×360° omnidirectional image based on no dead angle ODVS. The following two key issues are to be resolved at least: (1)two devices of no dead angle omnidirectional vision can be combined together as requested, and meet the unshaded requirement in structure design; (2)imaging in the transition zone of the two integrated ODVSs is continuous, and can meet certain image laws so as to fusing the video information.

3.2 Design of catadioptric mirror

In order to make imaging in the transition zone of the two integrated ODVSs continuous, this chapter adopts average angular resolution to design ODVS. There is a certain linear relationship between the point on the imaging plane and the incidence angle. The average angular resolution design method is following.

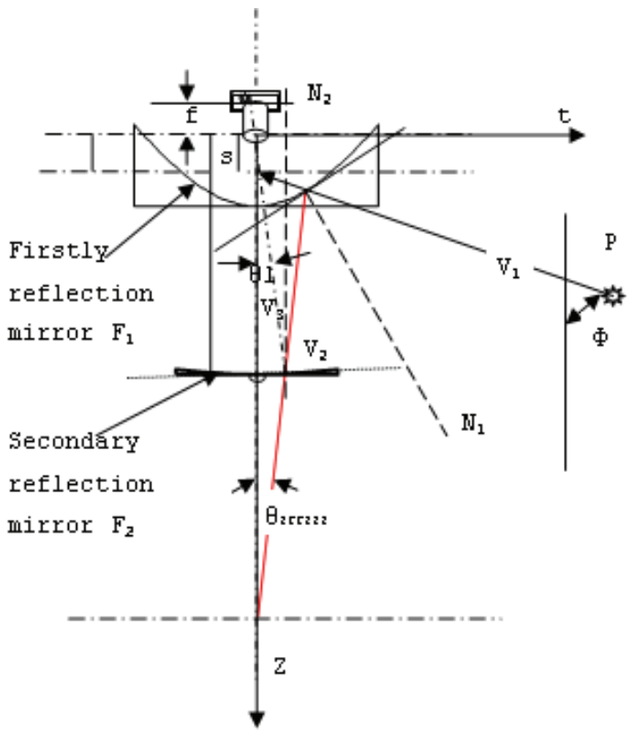

Fig. 3. Average angular resolution for two catadioptric imaging principle

The design of average angle resolution can be ascribed to the design of reflection mirror curve. As shown in Fig. 3, the incidence V_1 of a light source P reflects on the firstly reflection mirror $P_1(t_1,F_1)$, the reflected light V_2 reflects again on the secondary reflection mirror $P_2(t_2,F_2)$, the reflected light V_3 enters into the camera lens with the incidence angle of θ_1 then images on the camera unit (CCD or CMOS).

According to imaging principle, the angle between the first incidence V_1 and the spindle Z is ϕ, the angle between the first reflected light V_2 and the spindle Z is θ_2, the angle between the tangent through P_1 and the spindle t is σ, the angle between the normal and the spindle Z is ε the angle between the secondary reflected light V_3 and the main axis Z is θ_1, the angle between the tangent through P_2 and the spindle t is σ, the angle between the normal through P_2 and the spindle Z is ε_1. For these relations we can get the equation (1):

$$\begin{cases} \sigma = 180^0 - \varepsilon \\ 2\varepsilon = \phi - \theta_2 \\ \sigma_1 = 180^0 - \varepsilon_1 \\ 2\varepsilon_1 = \theta_1 - \theta_2 \end{cases} \tag{1}$$

Among them,

$$\tan\varphi = \frac{t_1}{F_1(t_1 - s)}, \tan\theta_2 = \frac{t_1 - t_2}{F_2 - F_1}, \tan\theta_1 = \frac{t_2}{F_2}$$

In the equation: F_1 is the firstly reflection mirror curve, F_2 is the secondary reflection mirror curve; s is the intersection of incidence V_1 and spindle Z.

Simplifying the equation by triangular relationship we can get:

$$F_1^{'2} - 2\alpha F_1^{'} - 1 = 0 \tag{2}$$

$$F_2^{'2} - 2\beta F_2^{'} - 1 = 0 \tag{3}$$

Among them,

$$\alpha = \frac{(F_1 - s)(F_2 - F_1) - t_1(t_1 - t_2)}{t_1(F_2 - F_1) - (t_1 - t_2)(F_1 - s)}, \beta = \frac{t_2(t_1 - t_2) + F_2(F_2 - F_1)}{t_2(F_2 - F_1) - F_2(t_1 - t_2)}$$

Solutions of (2), (3) can be:

$$F_1^{'} = \alpha \pm \sqrt{\alpha^2 + 1} \tag{4}$$

$$F_2^{'} = \beta \pm \sqrt{\beta^2 + 1} \tag{5}$$

Among them, $F_1^{'}$ is the differential of curve F_1, $F_2^{'}$ is the differential of curve F_2.

In order to make some certain linear relationship between the point on the imaging plane and the incidence angle, we need to build a linear relationship between the distance from pixel P to the spindle Z and the incidence angle ϕ, namely:

$$\phi = a_0 \cdot P + b_0 \tag{6}$$

In the equation: a_0, b_0 are arbitrary parameters.
If f is the focus of the camera unit, P is the distance from pixel to spindle Z, $P_2(t_2,F_2)$ is the reflex point on the secondary reflection mirror. According to imaging principle, we have:

$$P = f \cdot \frac{t_2}{F_2} \tag{7}$$

By substituting equation (7) into the equation (6), we can get:

$$\phi = a_0 \cdot (f \cdot \frac{t_2}{F_2}) + b_0 \tag{8}$$

The mirror curve satisfing equation (8) can meet the requirements of average angular resolution. According to the catadioptric principle by equation (8) we can get:

$$\tan^{-1}(\frac{t_1}{F_1 - s}) = a_0 \cdot (f \cdot \frac{t_2}{F_2}) + b_0 \tag{9}$$

We can get the numerical solutions F_1 and F_2 of the equation (2), (3),(9) by the forth-order Runge-Kutta algorithm (as shown in Fig. 4), so the firstly reflection mirror and secondary reflection mirror are of the average angular resolution.

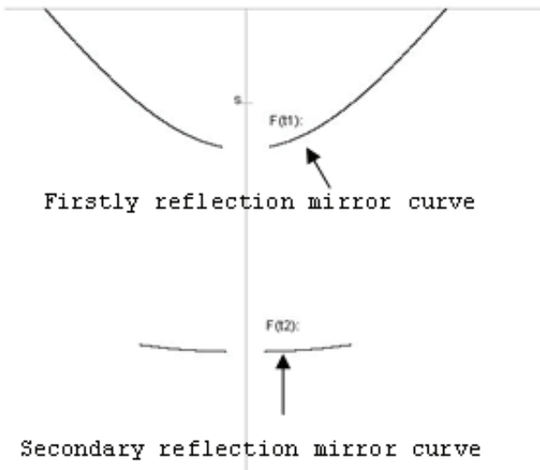

Fig. 4. Reflector curvilinear figure solution

3.3 Design of lens combination

From the ODVS viewpoint which is designed above, its view sheltered by the secondary reflection mirror that is video information before the secondary reflection mirror is invisible; in order to obtain this video information before the secondary reflection mirror. This chapter presents that a wide-angle lens is embedded in the center of the secondary reflection mirror. The wide-angle lens and the camera lens compose a combination lens device, as shown in Fig. 2. Fig. 5 shows the ubiety of the camera lens and the wide-angle lens. The wide-angle lens is configured in front of the firstly reflection mirror and in the secondary refection mirror. The central axises of camera lens, wide-angle lens, firstly reflection mirror and

secondary reflection mirror are configurated on the same axis line. The objects through the hole in the firstly reflection mirror image between the wide-angle lens and the camera lens (known as the first imaging point). This imaging point through the camera lens images at the camera component.

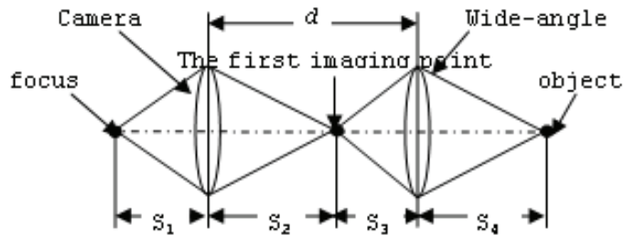

Fig. 5. Ubiety between camera lens and wide-angle lens

The focus of camera lens is f_1, the focus of wide-angle lens is f_2, the distance between camera lens and the camera lens focus is S_1, the distance between camera lens and the first imaging point is S_2, the distance from wide-angle lens to the first imaging point is S_3, and the distance from wide-angle lens to the object point is S_4, according to the lens imaging equation we can get the following relationships:

$$\frac{1}{f_1} = \frac{1}{S_1} + \frac{1}{S_2} \tag{10}$$

$$\frac{1}{f_2} = \frac{1}{S_3} + \frac{1}{S_4} \tag{11}$$

$$d = S_2 + S_3 \tag{12}$$

According to equation (12), as shown in Fig. 5 it should configure wide-angle lens with the distance d away from the firstly reflection mirror, and then we get the wide-angle imaging figure as the middle part of Fig. 5. But the present invention is configurating the wide-angle lens in the secondary reflection mirror, so the distance d between camera lens and the wide-angle lens is a constraint, and only by designing focus f_2 of wide-angle lens can we satisfy the requirements of equation (12). As shown in Fig. 4 taking the camera lens and the wide-angle lens into consideration, as a combination lens its focus can be got by

$$\frac{1}{f_3} = \frac{(f_1 + f_2 - d)}{f_1 f_2} \tag{13}$$

In addition, if the synthetic lens diameter is D, the magnification can be expressed by the following equation:

$$n = \frac{D}{f_3} \tag{14}$$

In order to make the view field of synthesized lens matching for the dead angle of ODVS, in this design it requires the following equation:

$$n = \frac{D}{f_3} = 2\theta_{1\max} \tag{15}$$

The $\theta_{1\max}$ is the maximum angle between the secondary reflected light V_2 and Z axis.

4. 360 °×360 ° field of view for the world's surface ODVS

4.1 ODVS with back to back configuration

According to the design above, each ODVS view scope can reach 240°×360° and have the same average angular resolution. So as long as fixing two ODVS back-to-back and making sure the two ODVS' axis lines overlap, the view scope of the two combined ODVSs of no dead angle full sphere device can reach 360°×360°. There are about 60° overlap field where the two can obtain images of the same spatial object at the same time, as shown in Fig. 6.

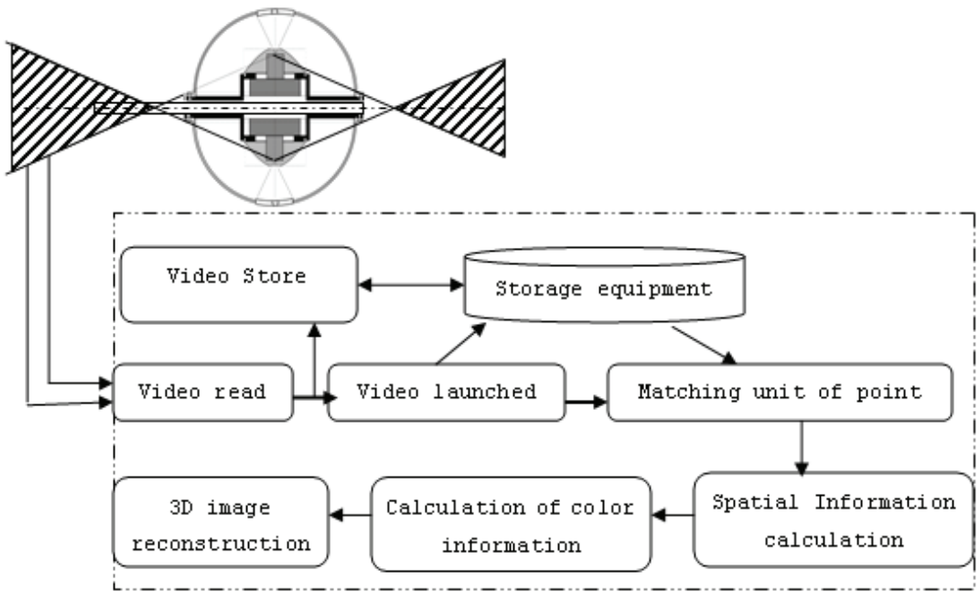

Fig. 6. Spherical ODVS with back to back and its image disposal flow

By combination of the camera lens and the wide-angle lens each ODVS captures image which locates in the centre of the entire image, as shown in Fig. 7(a), Fig. 7(b). Before unwrapping the omni-directional image we need to separate its central part alone; the calculation step at horizontal direction in the unwrapping algorithm is $\Delta\beta = 2\pi/l$; the calculation step at vertical direction is $\Delta m = \phi_{\max} - \phi_{\min}/m$; in the equation, $\phi_{\max}$ is the scene lighting incidence angle corresponding to the biggest effective radius (Rmax), $\phi_{\min}$ is the scene lighting incidence angle corresponding to the smallest effective radius (Rmin). The more details of the implement of the unwrapping are referred to Intelligent Omni-Directional Vision Sensors and Their Application.

As to the concrete realization, a connector is used to connect the two ODVSs together which are of the same average angular resolution and no dead angle, the camera's video cable and power cable are fetched out through the hole in the connector. as shown in Fig. 8. Each camera video cable of ODVS connects to video image access unit, because each camera of ODVS can get image information with view of 360°×240° and has the same average

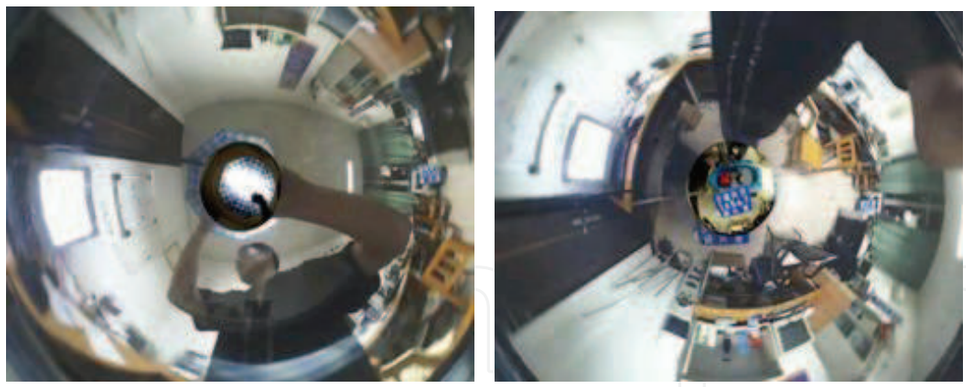

(a) Panoramic image of upside ODVS (b) Panoramic image of downside ODVS

Fig. 7. Panoramic images captured by spherical ODVS

Fig. 8. Full sphere ODVS with back to back configuration

Fig. 9. Video image from combination lens of downside & upside ODVS

angular resolution in the vertical (incidence angle) direction, it can realize image information fusion between the two ODVSs easily. Video access unit reads video information of each camera separately and stores in storage space (ODVStmp1, ODVStmp2), the two ODVS images are shown in Fig. 7(a), 7(b). Video image unwrapping unit reads the original video information in storage space (ODVStmp1, ODVStmp2) constantly, and splits the circular video images captured by the combination lens, as shown in Fig. 9. Then the obtained image of each ODVS is unwrapped by the unwrapping algorithm. ODVS image after unwrapping is shown in Fig. 10. In the unfolding figure the horizontal axis is azimuth, vertical axis is incidence angle. The splicing principle is azimuth alignment of the upper and the lower ODVS image, so the image point of the same material point in the two stitching

images are in a vertical line. In this chapter the spherical panorama after stitching does not include the overlapping part of the two ODVS, we only stitch when the incidence angle of ODVS is less than 90°. If you want to implement three-dimensional object point matching, spatial information calculation, three-dimensional image reconstruction, we need to calculate the overlapping part of the two ODVSs.

Fig. 10. Video unwrap mosaic image by two ODVS

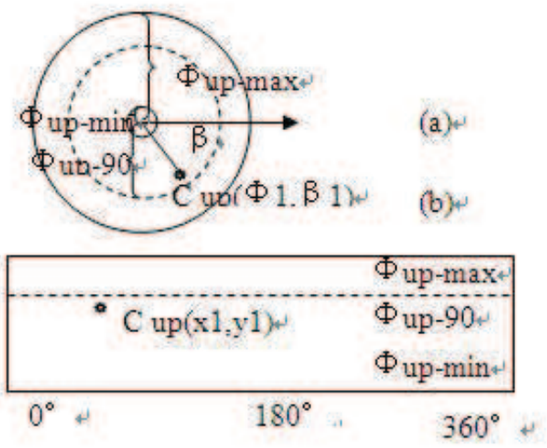

Fig. 11. Schematic diagram of panoramic vision photo graphed by upper ODVS

4.2 Match of the image point

Fig. 11 shows unwarped schematic diagram of upper ODVS. In unfolded image, x-axis expresses azimuth angle, y-axis expresses incidence angle. The principle of splicing is to match the azimuth angles of ODVS. It makes the same object from two unfolded images on the same vertical line in splicing image. If the longitudes of ODVS is justified during the design period, the ODVS can realiz the constraint of linear relationship in structure. After meeting the linear relationship, the problem search corresponding points in the entire unfolding iamge changes into searching in a vertical line. The reduction of search range provides foundation for the rapid match between point-to-point. From the viewpoint of latitude, if there is certain linear relation between the incidence angle and the pixels on image plane, the incidence angle of the ODVS can be calculated conveniently, and the problem can be simplified from searching corresponding points in a vertical line to a certain area of the vertical line. It should satisfy equation(16):

$$180° \le \phi_1 + \phi_2 \le 2\phi_{\max} \tag{16}$$

In this equation, ϕ_1 is the incidence angle of lower ODVS's imaging point, ϕ_2 is the incidence angle of upper ODVS's imaging point, $\phi_{\max}$ is the maximum incidence angle of ODVS imaging point called elevation.

We mark the upper ODVS as ODVSup and the lower ODVS as ODVSdown. Assume that the object point C is in the range of the binocular vision, its relevant point of imaging point in the panorama in ODVSdown is Cup (Φ1,β1) (shown in Fig. 11(a)), its coresponding object point in the spherical launched plane is Cup(x1,y1) (shown in Fig. 11(b)). Φup-max is the elevation when then incidence angle of ODVSup is the biggest, Φup-90 is the value 90° of the incidence angle of ODVSup, Φup-min is the depression angle when the incidence angle of ODVSup is the smallest.

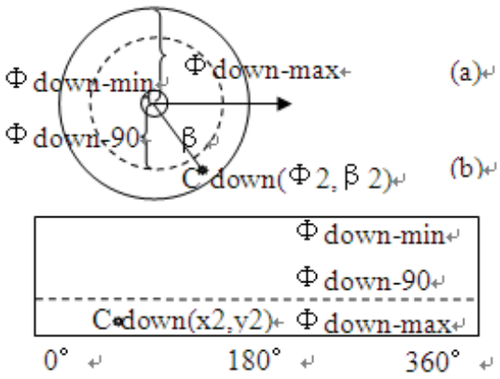

Fig. 12. Schematic diagram of panoramic vision photo graphed by lower ODVS

We can also know that object point C's relevant point of imaging point in the panorama in ODVSdown is Cdown(Φ2,β2)(shown in Fig. 12(a)), its object point in the spherical launched plane is Cdown(x2, y2) (shown in Fig. 12(b)).

The incidence angle bigger than 90° is called elevation while smaller is depression angle. In this chapter, we set the incidence angle of the ODVS as elevation, so it must have some area that both two ODVSs can reach which is named binocular vision scope. For the same object point in space, if it can be seen in the binocular vision scope, it must have two image relevant points (Cup(Φ1,β1) and Cdown(Φ2,β2)of the two panoramas of ODVS)which have the same azimuth angle β, that is, β1= β2.

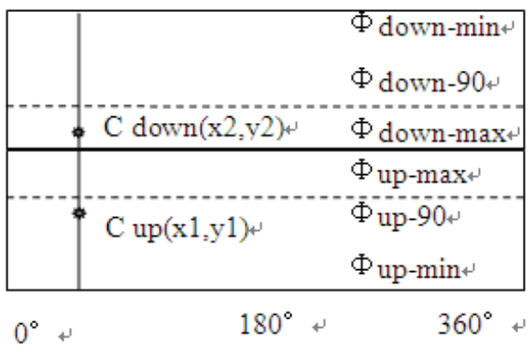

Fig. 13. Image point matching for two ODVSs

As a result, the X coordinate is the same corresponding to the spherical launched plane, that is x1=x2. So according to this principle, the azimuth angle of the two ODVS can be justified in the spherical launched plane, as shown in Fig. 13. Actually, the Fig. 13 is combination of the Fig. 11(b) and the Fig. 12(b), which can realize the justifying of the azimuth angles in the two spherical launched planes conveniently.

4.3 The coordinate of Gaussian sphere and central eye

Human-centered stereo omnidirectional vision is three dimension and high fidelity. We call the center of binocular vision's baseline as "central eye" which is used to describe the information of object point $c = C(r, \phi, \beta, R, G, B, t)$ in space. The meaning of each physical parameter is shown in Fig. 14.

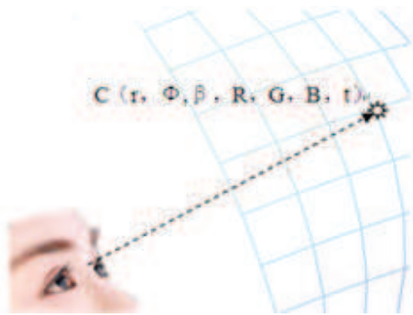

Fig. 14. Imaging point expression in Gaussian reference

The coordinate of central eye is used to be the origin o of Gaussian sphere coordinates in this design. We use seven parameters to describe the information of object point in space. r expresses the distance between origin o and object point; ϕ expresses the angle between Z axes and the line connecting origin o with object point; β expresses azimuth angle; R is the average value of central eye's red component; G is the average value of central eye's green component; B is the average value of central eye's blue component; t is time information. The equation(17) can express any object point in space,

$$c = C(r, \phi, \beta, R, G, B, t) \tag{17}$$

We adopt a scientific and uniform Gaussian sphere coordinate in binocular stereo vision system to express all object points by using seven physical parameters. It can provide a good technology foundation for model simplification and fast calculation in future. It also provides convenience for the follow-up geometric calculation.

4.4 Object point's spatial information and color information acquisition and calculation

The spatial information of object point is expressed by three parameters r, ϕ, β in Gaussian sphere coordinate. Because we use central eye as origin of Gaussian sphere coordinate, calculation of spatial information can be concluded to calculate the ubiety of object point and central eye. Among them r expresses the distance between origin o and object point. Compared with central eye, object point's longitude value is ϕ. Compared with central eye, object point's dimensionality value is β. According to the principle of binocular vision we can estimate the object point's depth information, as shown in Figure 15.

According to the imaging principle of binocular vision, we can get the distance from object point to the central eye that is depth information by only obtaining the incidence angle of object point of ODVS Φ1 and Φ2. Because two ODVSs are combined together by back-to-back manner, Φ1 and Φ2 can be counted by equation (18), (19):

$$\phi_1 = \phi_{\min} + (\phi_{\max} - \phi_{\min}) / m \cdot (m - y_1) \tag{18}$$

$$\phi_2 = \phi_{\min} + (\phi_{\max} - \phi_{\min}) / m \cdot y_2 \tag{19}$$

In the equation, m is the height of unfolded image; y_1, y_2 is the match point on y-axis in two unfolded images; $\phi_{\min}$ is the minimum incidence angle; $\phi_{\max}$ is the maximum incidence angle.

According to the triangular relationship, we can get the distance r between origin o and point C,

$$\begin{aligned} r = \overline{OC} &= \sqrt{\overline{AC}^2 + (dc/2)^2 - 2\overline{AC}(dc/2)\cos A} \\ &= \sqrt{[\frac{dc}{\sin(A+B)} \bullet \sin B]^2 + (dc/2)^2 - \frac{dc^2}{\sin(A+B)} \bullet \sin B \cos A} \\ &= \sqrt{[\frac{dc}{\sin(\phi 1+\phi 2)} \bullet \sin \phi 1]^2 + (dc/2)^2 + \frac{dc^2}{\sin(\phi 1+\phi 2)} \bullet \sin \phi 1 \cos \phi 2} \end{aligned} \tag{20}$$

In the equation A=180°-Φ2, B=180°- Φ1, dc is the distance between ODVSup's viewpoint and ODVSdown's viewpoint.The incidence angle Φ can be counted by the equation (21):

$$\phi = \arcsin(\frac{dc}{2r}\sin\phi_2) + \phi_2 - 180^\circ \tag{21}$$

Φ is the incidence angle of object point; dc is the distance between point A and point B in binocular system; r is the distance between object point and central eye; Φ2 is the incidence angle of ODVSup. Another parameter β can choose from one of the two ODVS's azimuth angle. t is the time from computer system.

The average value of each color components R, G, B of matching points of two unfolded image are adopted as central eye's color coding. First we obtain color components R_{ODVS1}, R_{ODVS2}, G_{ODVS1}, G_{ODVS2}, B_{ODVS1} and B_{ODVS2} of matching points of unfolded image, then the average value of each color component is counted as central eye's color coding. The equation is shown as follows:

$$\begin{aligned} R &= \frac{R_{ODVS1} + R_{ODVS2}}{2} \\ G &= \frac{G_{ODVS1} + G_{ODVS2}}{2} \\ B &= \frac{B_{ODVS1} + B_{ODVS2}}{2} \end{aligned} \tag{22}$$

In the equation, R is the average value of red component; R_{ODVS1} is red component of ODVS one; R_{ODVS2} is red component of ODVS two; G is the average value of green component; G_{ODVS1} is green component of ODVS one; G_{ODVS2} is green component of ODVS two; B is the

average value of blue component; B_{ODVS1} is green component of ODVS one; B_{ODVS2} is blue component of ODVS two; the value range is 0~255.

4.5 Depth accuracy

The vertically-aligned binocular omnistereo systems have two viewpoints and a fixed baseline. For the stereo matching between the two converted panoramic views, any conventional algorithms is applicable. Once correspondence between image points has been established, depth calculation in both spherical and cylindrical panorama is easily counted by simple triangulation in equation (20). And the depth resolution mainly depends on camera resolution, the length of baseline.

$$\partial r = f(\frac{r^2}{dc})\partial\phi \tag{23}$$

Where, r is the distance between viewing object and Binocular Omnistereo Vision Sensor, dc is the length of baseline, $\partial\phi$ is similar to the camera resolution. It seems that larger baseline and higher camera resolution will get better depth accuracy. And depth estimation error is proportional to the 2 power of the distance between viewing object and Binocular Omnistereo Vision Sensor. The depth accuracy of the V-binocular omnistereo is isotropic in all directions, and the epipolar lines is simply vertical lines in omnidirectional image.

5. Experimental results

5.1 Full sphere view and without dead angle

Full sphere ODVS is shown in Fig. 8, the two ODVSs are fixed together back to back by a connector. Its view scope is same as the full sphere camera device as shown in Fig. 1(b). The original panoramic images of the upper and the lower ODVS are shown in Fig. 7(a) and Fig. 7(b). The center part of the image is the imaging of wide-angle lens, that is, the dead angle parts of the upper and lower ODVS of the secondary reflection mirror shown in Fig. 9(a) and 9(b). In Fig. 7(b) the ship brand is partly sheltered by the secondary reflection mirror of the lower ODVS, but the combination lens can also obtain the ship brand video information, shown in Fig. 9(b); Similarly, the lattice umbrella is partly sheltered by secondary reflection mirror of the upper ODVS, however, the lens combination can also obtain the lattice umbrella video information shown in Fig. 9(a).

By splicing the unwrapping images of the panoramic image Fig. 8(a) and 8(b) the fusion of the video images is shown in Fig. 10. From the experimental results of image processing we can see the full sphere ODVS in this article can be real-time and capture the entire 360°×360° spherical images within the surveillance video. Further improvements in the future are to solve the problem of fusion between wide-angle lens and ODVS image, using 360°×360° full sphere ODVS to implement three-dimensional reconstruction and ranging.

5.2 Measuring depth of viewing object

In order to get better depth accuracy range for special application requirements, we carry out experiments to measure depth of viewing object using V-binocular stereo ODVS of back-to-back configuration.

The panoramic images obtained by binocular stereo ODVS are transmited to computer through two USBs. After it computer will process these images, match the object points, and

measure the depth of object point. Fig. 16 is shown the experimental device and environment a panoramic image of both the frames of upper ODVS and lowwer ODVS graphed by V-binocular stereo ODVS with back-to-back configuration, its sphere panoramic image resolution is 640×480, unwrapped panoramic image resolution is 1280×200. Experiments measuring depth between viewing object (in red cross mark) and central eye(origin O) are carried out using the binocular stereo ODVS experiment device, from short distance to long distance respectively. Fig. 17 shows parts of experiments for matching the object point and measuring the depth of object point. The software is developed by Java and operating system is Windows XP.

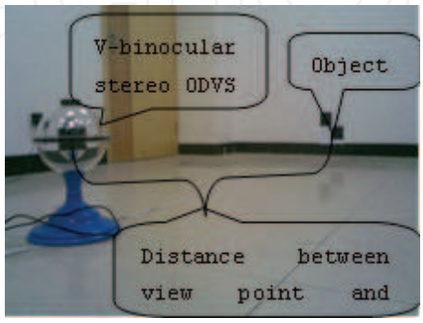

Fig. 16. Experiments for measuring depth of object

Fig. 17. Experiments for matching the object point and measuring the depth of object point

Actual depth (cm)	Up image plane coordinates $C_{up}(x_1, y_1)$	Angle of incidenceΦ1 (degree)	Down image plane coordinates $C_{down}(x_2, y_2)$	Angle of incidenceΦ2 (degree)	Depth estimation (cm)	Error ratio (%)
30.00	618,47	98.81	618,151	98.26	33.08	10.28
40.00	618,52	97.43	618,143	96.02	42.25	5.63
50.00	616,57	96.02	616,138	94.56	54.05	8.11
60.00	618,60	95.15	618,136	93.97	62.99	4.98
70.00	617,62	94.56	617,134	93.37	72.73	3.91
80.00	616,62	94.56	616,131	92.45	82.54	3.18
90.00	616,64	93.97	616,130	92.14	95.21	5.79
100.00	617,66	93.37	617,129	91.83	100.50	0.50
110.00	617,66	93.37	617,129	91.83	112.64	2.40
120.00	616,66	93.37	616,128	91.52	120.16	0.14
130.00	617,67	93.06	617,128	91.52	128.50	-1.15
140.00	616,67	93.06	616,127	91.21	138.44	-1.12
150.00	618,67	93.06	618,127	91.21	138.44	-7.71
160.00	619,68	92.76	619,127	91.21	149.68	-6.45
170.00	616,69	92.45	616,127	91.21	162.99	-4.12
180.00	619,69	92.45	619,126	90.89	179.38	-0.35
190.00	616,69	92.45	616,126	90.89	179.38	-5.59
200.00	617,70	92.14	617,126	90.89	198.92	-0.54
210.00	619,70	92.14	619,126	90.89	198.92	-5.28
220.00	618,71	91.83	618,124	90.25	298.44	35.65
230.00	617,71	91.83	617,124	90.25	298.44	29.76
240.00	616,71	91.83	616,124	90.25	298.44	24.35
250.00	617,71	91.83	617,124	90.25	298.44	19.38

Table 1. Experimental results of measuring depth between view point and object from 30cm to 250cm using V-binocular ODVS with Back-to-Back configuration in Fig. 16

Actual depth (cm)	Up image plane coordinates $C_{up}(x_1, y_1)$	Angle of incidenceΦ1 (degree)	Down image plane coordinates $C_{down}(x_2, y_2)$	Angle of incidenceΦ2 (degree)	Depth estimation (cm)	Error ratio (%)
100.00	617,67	93.37	617,129	91.83	100.50	0.01
200.00	617,70	92.14	617,126	90.89	198.92	-0.54
300.00	617,71	91.87	617,123	89.93	359.08	19.69
400.00	617,72	91.40	617,120	88.96	462.75	15.69
500.00	617,73	91.12	617,118	88.30	645.85	29.17
600.00	617,70	92.14	617,124	90.25	969.43	61.57
700.00	617,71	91.83	617,124	90.25	1113.63	59.09
800.00	618,71	91.83	618,123	89.93	1316.21	64.53
900.00	617,71	91.83	617,129	91.83	1610.93	78.99
1000.00	618,72	91.52	618,122	89.61	2055.70	105.57
1100.00	617,72	91.52	617,125	90.72	2884.77	162.25

Table 2. Experimental results of measuring depth between view point and object from 100cm to 1100cm using V-binocular ODVS with Back-to-Back configuration in Fig. 16

Table 1 are experimental resluts of measuring depth between view point and object with distance from 30cm to 250cm, and Table 2 are experimental resluts of measuring depth between view point and object from 100cm to 1100cm, both using V-binocular ODVS with Back-to-Back configuration, the baseline length of which is 9.80cm, in Fig. 16.

6. Discussion

In order to obtain real-time 360°×360° entire full sphere view scope video, this chapter presents a secondary catadioptric principle and structure of ODVS, and designs a catadioptric mirror, use fourth-order Runge-Kutta algorithm to obtain numerical solution of the reflection mirror by the design method of combination lens integrating ODVS with wide-angle lens to eliminate the inherent dead angle of the original ODVS, and then fixes the two ODVS devices without dead angle back to back, finally stitches the 360°×360° video image seamlessly by unwrapping algorithm. The experimental results show that the design of ODVS device can obtain real-time 360°×360° view scope video image. The software which we develop for the full sphere ODVS to do experimental studies runs in the operation system of Windows XP with CPU of 1.7Celeron and 512M RAM. When the resolution of camera is 640×480, the system can handle 15 frames per second, and basically satisfy the requirements of real-time video data acquisition.

Because each ODVS of the composition of full sphere ODVS adopts average angular resolution to design, the parameters of the two ODVS fixed back to back are fully consistent and the point of imaging plane and the incidence angle has a linear relationship, thus it can make sure the imaging of transition zone of the integrated ODVS is continuous.

For the reflection mirror design, this chapter uses Runge-Kutta algorithm to obtain the numerical solution of the reflection mirror of ODVS and validates the catadioptric mirror by the simulation experiment. This method can guide design of ODVS mirror, and provide a theoretical support to ODVS reflection mirror design.

Fig. 10 shows the unwrapping stitching image exists stitching error. The reason is that the central axis of the upper and the lower ODVS has error in manufacturing and assembly processing. It is difficult to ensure the two ODVS fixed back to back on the same axis line,

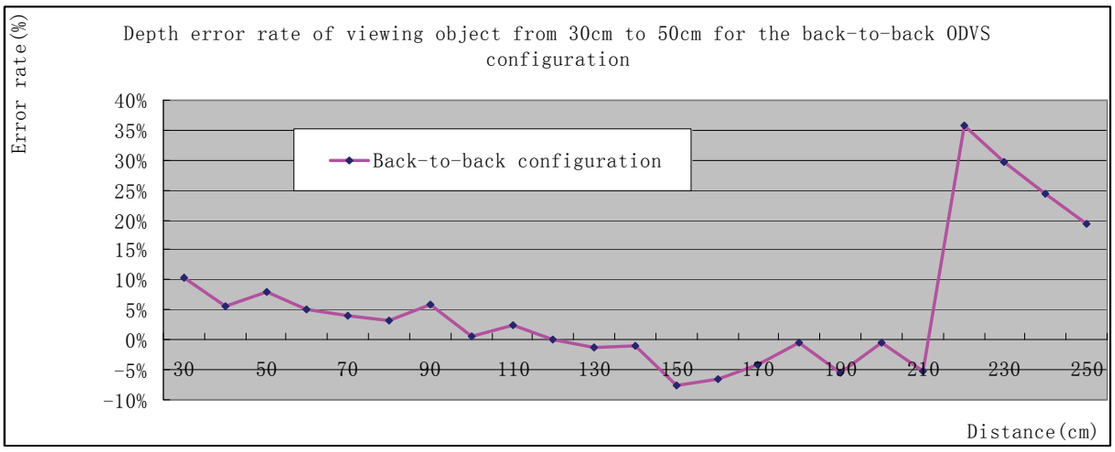

Fig. 18. Depth estimate error rate of viewing object from 30cm to 250cm for the V-binocular ODVS with back to back configuration

but this problem can be solved by ensuring the same axis angle when assembling in the technic schedule.

Depth error analysis of distance calculation is shown as Fig. 18. According to the principle of binocular stereo vision the position of object can be measured exactly. But the image is not continuous when it is obtained by imaging unit. The image is discrete data which takes pixel as a unit. There is minimum resolution ratio error in measurement due to camera's resolution. This problem can be improved by using high resolution camera.

According to the measurement results, depth estimation error will increase with the increase of distance from target object. Because in the same direction when the measuring distance increases, the variable quantity of incidence angle in two ODVS Φ1 and Φ2 is becoming smaller, and the incidence angle of upper and lower ODVS both tend to 90°. It makes the distance from target object of the equation (20) very sensitive to the change of incidence angle.

7. Conclusion

A novel dynamic omnistereo approach is presented by which viewpoints of two omnidirectional camera can form optimal stereo configuration for localizing moving objects. Further extension is made to the concept of omnidirectional imaging from viewer-centered to object-centered representation, thus it allows establishing omnidirectional models of large objects or even our planet. Numerical analysis is given on omnidirectional representation, epipolar geometry and depth error characteristics, which could be very useful for the research and applications of omnidirectional stereo vision.

The beneficial effects of 360°×360° full sphere ODVS designed in this chapter are mainly reflected in: 1)It can obtain real-time 360°×360° omni-directional 3D video images, then by geometry calculation get the whole panoramic image of the monitoring sphere. The monitor tracking objects will never be lost; 2)It uses the average angular resolution for the ODVS design. The whole image of monitor sphere is not heteromorphic solving the problem of catadioptric ODVS image distortion. It provides a complete theoretical system and model for the fast-moving target real-time tracking in large space. 3)Because each ODVS of the composition of full sphere ODVS uses the average angle resolution to design, the parameters of the two ODVS cameras are fully consistent with good symmetry. In the spherical coordinates the real-time video image obtained can rapidly match point and point providing more convenience for the subsequent three-dimensional image process. 4)The ODVS design uses catadioptric technology, so it exists the problem of fixed focus, the clarity is same in any area of the image; 5)It Uses a secondary catadioptric imaging technology and easily implement miniaturization. It can be widely used in military reconnaissance, aviation and navigation, virtual reality and so on .

8. Reference

Peleg, S.; Ben-Ezra, M. & Pritch, Y. (2001). *Omnistereo: Panoramic Stereo Imaging* [J].IEEE Transaction on Pattern Analysis any Machine Intelligence, 2001, 23(23): 279–290

Matthew Brown & David G. Lowe. *Automatic panoramic image stitching using invariant features*[J].International Journal of Computer Vision, 2007,74 (1):59–73.

Shum H Y & Szeliski R.(2000) *Systems and experiment paper: construction of panoramic image mosaics with global and local alignment*[J].International Journal of Computer Vision, 2000,36(2):101–130.

Nalwa Vishvjit Singh (Holmdel, NJ). *Panoramic Viewing System with a Composite Field of View* [P].United States Patent.6700711.Mar 2, 2004.

Peleg S & Herman J. *Panoramic mosaics by manifold projection*[J]. Proc.of IEEE conference on CVPR [C].San Juan.Puerto Rico,1997,pp.338-343.

David McCutchen. *Immersive imaging method and apparatus*[P].US Patent.6141034. October 31, 2000.

TANG Yi-ping. *Omni Directional Vision Sensors without dead angle*. Chinese Patent No.200710066757.0, .pages 446-451,2007-07-25.

TANG Yi-ping et al. *Research on Intelligent Omni-Directional Vision Sensors and Their Application*, CHINESE JOURNAL OF SENSORS AND ACTUATORS, Vol. 20, No. 6, pages 1316~1320,2007.

Koyasu H & Miura J,Shirai Y.(2002). *Recognizing moving obstacles for robot navigation using real-time omnidirectional stereo vision*. Journal of Robotics and Mechatronics,2002,14(2):147-156.

SU Lian-Cheng & ZHU Feng. *Design of a Novel Omnidirectional Stereo Vision System* [J]. ACTA AUTOMATICA SINICA ,2006,32(1):69-74.

Tomas Pajdla & Tomas Svoboda. *Epipolar Geometry for Central Catadioptric Cameras*[J]. International Journal of Computer Vision,2002,49(1):23–37.

Zhu Z et al. *Panoramic virtual stereo vision of cooperative mobile robots for localizing 3D moving objects*. Proceedings of IEEE Workshop on Omnidirectional Vision – OMNIVIS'00, Hilton Head Island,pages 29-36,2000.

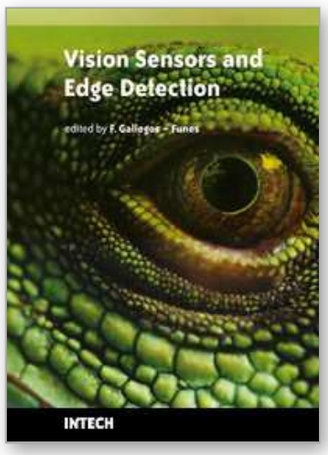

Vision Sensors and Edge Detection
Edited by Francisco Gallegos-Funes

ISBN 978-953-307-098-8
Hard cover, 196 pages
Publisher Sciyo
Published online 12, August, 2010
Published in print edition August, 2010

Vision Sensors and Edge Detection book reflects a selection of recent developments within the area of vision sensors and edge detection. There are two sections in this book. The first section presents vision sensors with applications to panoramic vision sensors, wireless vision sensors, and automated vision sensor inspection, and the second one shows image processing techniques, such as, image measurements, image transformations, filtering, and parallel computing.

INTECH
open science | open minds

InTech Europe
University Campus STeP Ri
Slavka Krautzeka 83/A
51000 Rijeka, Croatia
Phone: +385 (51) 770 447
Fax: +385 (51) 686 166
www.intechopen.com

InTech China
Unit 405, Office Block, Hotel Equatorial Shanghai
No.65, Yan An Road (West), Shanghai, 200040, China
中国上海市延安西路65号上海国际贵都大饭店办公楼405单元
Phone: +86-21-62489820
Fax: +86-21-62489821

IntechOpen